HHS Public Access

Author manuscript

Sci Immunol. Author manuscript; available in PMC 2017 April 01.

Published in final edited form as:

Sci Immunol. 2016 October ; 1(4): . doi:10.1126/sciimmunol.aah3732.

Bidirectional intragraft alloreactivity drives the repopulation of human intestinal allografts and correlates with clinical outcome

Julien Zuber[1,8], **Brittany Shonts**[#1], **Sai-Ping Lau, BSc**[#1], **Aleksandar Obradovic**[1], **Jianing Fu**[1,8], **Suxiao Yang**[1,8], **Marion Lambert**[2], **Shana Coley**[1,3], **Joshua Weiner**[1,4], **Joseph Thome**[1,5], **Susan DeWolf**[1,8], **Donna L. Farber**[1,4,5], **Yufeng Shen**[6], **Sophie Caillat-Zucman**[2], **Govind Bhagat**[3], **Adam Griesemer**[1,4], **Mercedes Martinez**[7], **Tomoaki Kato**[4], and **Megan Sykes**[1,4,5,8,*]

[1]Columbia Center for Translational Immunology, Columbia University Medical Center, New York, USA

[2]INSERM UMR1149, Hôpital Robert-Debré, Paris, France

[3]Department of Pathology and Cell Biology, Columbia University, New York, USA

[4]Department of Surgery, Columbia University, New York, USA

[5]Department of Microbiology & Immunology, Columbia University, New York, USA

[6]Center for Computational Biology and Bioinformatics, Columbia University Medical Center, New York, USA

[7]Department of Pediatrics, Columbia University, New York, USA

[8]Department of Medicine, Columbia University, New York, USA

[#] These authors contributed equally to this work.

Abstract

A paradigm in transplantation states that graft-infiltrating T cells are largely non-alloreactive "bystander" cells. However, the origin and specificity of allograft T cells over time has not been investigated in detail in animals or humans. Here, we use polychromatic flow cytometry and high throughput TCR sequencing of serial biopsies to show that gut-resident T cell turnover kinetics in human intestinal allografts are correlated with the balance between intra-graft host-vs-graft (HvG) and graft-vs-host (GvH) reactivities and with clinical outcomes. In the absence of rejection, donor T cells were enriched for GvH-reactive clones that persisted long-term in the graft. Early

[*] To whom correspondence should be addressed: Megan Sykes, MD, Columbia Center for Translational Immunology, 650 West 168th street, Black Building 1512, (Mailbox 127), New York, 10032, Tel: 212.304.5696 Fax: 646.426.0019 megan.sykes@columbia.edu.

Author contributions: JZ, MM, TK and MS designed the study; JZ, BS, SPL, JF, ML, SC, JW performed the experiments. JZ, BS, SPL, JF, SY, JT, AG, MM collected the data. JZ, BS, SPL, AO, ML, SDW, DF, YS, SCZ, GB, AG, MM, TK, MS performed data analysis. YS (senior biostatistician) and AO wrote the codes to identify and track the alloreactive clones and performed the statistical analyses. JZ, AO, MS wrote the final report. All authors contributed to the editing of the final report. All authors agreed all of the content of the submitted manuscript.

Competing interests: The authors did not declare any competing interests.

Data and material availability: Raw TCR sequences data are freely accessible through the following URL: immunoseq.com (username: projectreview@adaptivebiotech.com; password: ProjectReview). The codes used to analyze TCR sequences are available and can be uploaded from a public github repository (https://github.com/Aleksobrad/TCR-analysis).

expansion of GvH clones in the graft correlated with rapid replacement of donor APCs by the recipient. Rejection was associated with transient infiltration by blood-like recipient CD28+ NKG2D^{Hi} CD8+ alpha beta T cells, marked predominance of HvG clones, and accelerated T cell turnover in the graft. Ultimately, these recipient T cells acquired a steady state tissue-resident phenotype, but regained CD28 expression during rejections. Increased ratios of GvH to HvG clones were seen in non-rejectors, potentially mitigating the constant threat of rejection posed by HvG clones persisting within the tissue-resident graft T cell population.

Introduction

Small bowel transplantation is complicated by high rates of rejection(*1*), infection and, in 5-9% of cases, graft-vs-host disease(*2*), resulting in approximately 50% patient 5-year survival rates. Large numbers of donor lymphohematopoietic cells are transferred within these grafts(*2*). This large load of passenger donor-derived T cells combined with reductions of recipient T cell mass may promote Graft-versus-Host (GvH) disease (GVHD)(*3*). Conversely, donor-specific antibodies (DSA) and associated intractable rejections have emerged as leading causes of intestinal allograft failure(*1*) and pre-transplant DSAs are associated with accelerated clearance of graft-derived circulating donor cells(*4*) and lower rates of GVHD(*3*) after intestinal transplantation. We hypothesized that clinical outcomes might largely reflect the balance between host-versus-graft (HvG) and GvH reactivities.

Long-lived tissue-resident memory T cells (T_{RM}) have been implicated in murine and human tissue-specific inflammatory disease(*5*). T_{RM} display hallmark phenotypic markers (CD103, CD69)(*6*), demonstrate tissue-specific T-cell repertoires(*5, 7*) and persist long-term in mucosal tissues(*8, 9*). However, little is known about how HvG and GvH responses influence the turnover, phenotype and repertoire of tissue-resident T-cell populations following transplantation. Studies in mice(*10*) and humans(*11*) have indicated that recipient-derived T cells repopulate the GALT (Gut-Associated Lymphoid Tissues) of intestinal allografts early after transplantation. However, the turnover rate of mucosal T cells after intestinal transplantation has been investigated in only a few patients(*12*) in cross-sectional studies(*11*), without phenotype or repertoire analysis(*11, 12*). We took advantage of serial protocol biopsies in intestinal transplant recipients to address the hypothesis that recipient cells would replace the donor leukocytes rapidly in the presence of rejection and that homeostatic leukocyte turnover could be measured in the absence of rejection. Moreover, we utilized a novel method of identifying and tracking the alloreactive T cell repertoire to determine the role of GvH and HvG clones in this turnover. Our studies revealed that donor T cells often persist much longer than previously thought in non-rejecting intestinal allografts. The replacement rate of donor T cells varied greatly between patients, depending on the presence or absence of rejection. Recipient T cells repopulating the graft ultimately acquire a tissue resident phenotype. Contrary to the current paradigm(*13*), our alloreactive TCR tracking method allowed us to demonstrate that the majority of graft-infiltrating recipient T cell clones during pure cellular rejection are in fact donor antigen-specific and that the balance of *in situ* GvH and HvG responses correlates with the kinetics of graft leukocyte turnover. Graft-resident GvH clones preexisted in donor lymphoid organs as circulating memory cells with an intestinal mucosa counterpart.

Results

Greatly variable graft lymphocyte turnover rates.

Using recipient and/or donor-specific monoclonal antibodies (Table S1) in combination with a pan-HLA class I mAb, the phenotypes and origins of intra-epithelial lymphocyte (IEL) and lamina propria lymphocyte (LPL) populations were investigated with multicolor flow-cytometry. Single cell suspensions were obtained from 183 fresh ileum graft biopsies, from 14 intestinal transplant patients (Fig. 1A-B, S1-2, and Table S2), including 9 patients followed from transplantation to last follow-up (Fig. 1B, S2 lower panel). $CD45^{-}$ non-hematopoietic cells, found mainly in IELs and assumed to be epithelial cells, remained of donor origin as expected (Fig. 1A-B, S2). In contrast, recipient T cell replacement occurred over time (Fig. 1B), but with highly variable kinetics between patients (Fig. 1B-C, S2). Overall, recipient replacement rates were less uniform and slower for CD45+ CD3+ T cells than for CD56+ CD3− NK/ILC cells (Fig. 1C) and donor graft lymphocytes persisted much longer than previously reported (Fig. 1 B-C and S2)(*11, 12*).

Faster replacement rate of gut-resident T-cell subsets in rejecting intestinal allografts.

We hypothesized that uncontrolled rejection would hasten the turnover of gut-resident T cells. We thus analyzed the chimerism of CD3+ γδ TCR-negative (αβ) CD4 and CD8 T cell populations according to the occurrence of biopsy-proven rejection and donor-specific antibody (DSA) (Fig. 1D). Seven patients experienced early rejections, within 90 days after transplantation including four with high titer (MFI>2000) anti-HLA class I and II DSA and histological features of mixed (cellular and antibody-mediated) rejection (Fig. 1D). Low levels of recipient chimerism among $CD4^{+}$ and $CD8^{+}$ αβ TCR^{+} IELs and LPLs during the first 45 days were significantly associated with the absence of biopsy-proven rejection (Fig. 1E, Table S3). Over time, cell replacement rates in the graft were significantly faster for CD4+ and CD8+ αβTCR+ LPL and IEL over the first 3 and 6 months post-transplant in patients with mixed rejection compared to those without (Fig. 1F and S3). Of note, recipient chimerism that peaked at the time of early pure T-cell-mediated rejection (TCMR), especially in CD4+ IEL, then returned to baseline after rejection resolution (Fig. 1F). In contrast, recipient chimerism peaked at a greater level in mixed rejection compared to TCMR, and remained a way greater than prior rejection even after treatment (Fig. 1F). Differences in treatment-induced tissue lymphodepletion did not account for these differences, as absolute CD3+ IEL counts on immunostained biopsy sections were similar in both groups following anti-thymoglobulin induction and at 3 months (Fig. S4). Together, our findings demonstrate that strong anti-donor immune responses accelerated recipient replacement of donor αβ T lymphocytes in human intestinal allografts.

Recipient T cells involved in rejection initially exhibit a different phenotype from those arising from physiological turnover

Human mucosal-resident T cells show reduced expression of CD28, especially on CD8 cells, and high expression of CD103 and CD69 compared to peripheral blood cells(*6, 14*). We analyzed IEL and LPL phenotypes from171 ileal graft biopsies from 9 intestinal transplant recipients (Fig. 2) and from 10 ileum specimens obtained from deceased organ donors (Fig. S5A and Table S2). Donor-derived IEL and LPL exhibited roughly the same phenotypic

features as those from organ donors (Fig. 2A and S5A). However, the phenotype of recipient-derived IEL and LPL cells isolated from early biopsies differed significantly from that of donor cells (Fig. 2A-C), displaying an intermediate phenotype between those of blood-borne and gut-resident T cells (Fig. 2A). Recipient T cells eventually acquired tissue-resident phenotypic markers (Fig. 2B-C).

While CD28 expression among recipient IEL T cells was initially higher than that of resident donor T cells even in the absence of rejection (Fig. 2C, 2E), a significantly greater proportion of recipient CD8+ IEL T cells expressed CD28 within a week of rejection episodes than in biopsies more temporally removed from rejections (Fig. 2D-E). Notably, CD28+ CD8+ IELs from late rejections expressed high levels of CD103 and CD69, like their CD28− counterparts (Fig. 2D). In the context of gut inflammation, up-regulation of NKG2D by CD8+ IELs, with increased expression of its ligands, has been correlated with enhanced cytotoxic potential(*15, 16*). While most recipient CD8+ IELs expressed less NKG2D than peripheral blood CD8 T cells, similar to donor CD8+ IELs and those from organ donors (Fig. S5B), CD8+ CD28+ recipient IELs exhibited high NKG2D expression in rejecting biopsies (Fig. S6A). In parallel, the epithelium of rejecting biopsies expressed much higher levels of the NKG2D ligand MICA than non-rejecting grafts or normal duodenum (Fig. S6B). Taken together, these data suggest that recipient-derived CD28+ $NKG2D^{Hi}$ CD8+ IEL play a role in graft rejection, whose late forms may have a T_{RM} component.

Origin and turnover of the ileal T cell repertoire following transplantation.

High throughput TCRβ CDR3 analysis was performed on 18 ileal biopsies, including 6 with overt rejection, from 7 intestinal transplant recipients (Fig. 3A). As expected, complete replacement of donor graft-resident T cells by the recipient was accompanied by extensive repertoire turnover (Pt9, Pt10 T1-2, Pt14 T1-3), whereas the TCR repertoire was more conserved over time when the graft-resident T cells were mostly of the same origin (donor vs recipient) across different biopsies (Fig. 3B-C, S7). Among the clones in the biopsies that could be mapped to pre-transplant donor or recipient lymphoid samples (Table S4), we examined repertoire overlap between early and late biopsies. Considering that different sites were biopsied at different time points, donor-derived T cells exhibited a remarkably stable repertoire as long as they were maintained in the graft, as reflected by the high repertoire overlap over periods of 55-200 days in patients that showed little T cell replacement by the recipient in this period (Pts 7, 13, 15, Fig. 3B, C, D). In contrast, recipient cells from the same biopsies displayed much greater turnover, but still with significant overlap between early and late time points (Fig. 3D-F). In Patient 14, for instance, 19.5% of the 773 clones identified as derived from the recipient in POD16 biopsy were shared with those detected at POD156 (Fig. 3E). In terms of cumulative frequency, 21.3 and 67.6% of the recipient clones found in the POD156 biopsy (T3') overlapped with recipient clones from POD16 (T2') and POD226 (T4') biopsies, respectively (Fig. 3F). Similarly for all patients, recipient cell repertoire became more stable over time, following complete replacement of donor lymphocytes by the recipient (Fig. 3F, Pts 4, 10 and 14). Together with the finding that recipient cells eventually expressed high levels of CD69 (Fig. 3G), these data suggest that

the first T cells entering the graft were mainly CD69− effector cells with a short life span, a minor subset of which gave rise to recipient-derived long-lasting CD69+ T_{RM}.

HvG-reactive clones accumulate in rejecting biopsies.

We hypothesized that rejection-associated increases in recipient T cell repopulation of the graft reflected infiltration of HvG clones. To test this hypothesis, we identified (pre-transplant) and tracked the donor-reactive TCR repertoire in post-transplant biopsies using the high-throughput sequencing approach we recently described (Table S4)(*17*).

We investigated 5 biopsies with early rejection, from days 12 to 24 (Fig. 3A and 4A). HvG-reactive clones were highly enriched relative to non-HvG-reactive clones in the biopsies with rejection compared to pre-transplant peripheral lymphoid samples. HvG clones subsequently declined, yet persisted at lower frequency, after the resolution of rejection (Fig. 4A). Notably, the greatest enrichment in HvG clones (up to 80% of recipient-mappable clones), both in CD4 and CD8 T cells, was observed in biopsies with pure T-cell-mediated rejection. Patient 15, who remained free of rejection within the first 3 months post-transplant, showed enrichment of HvG clones in two early biopsies (POD27 and POD55) compared to pre-transplant lymphoid tissues, but to a lesser degree than those in patients with early rejections (Fig. 4A). The increased frequency of HvG clones was less compelling in late rejection and importantly did not change significantly after successful treatment (Fig. 4A). In addition, blood TCR repertoire was analyzed at the time of rejection before any treatment in one patient and showed strikingly less enrichment for HvG-reactive clones than was seen in the rejecting graft (Fig. 4B). Thus, we concluded that HvG clones accumulated within the graft at the time of early rejection and then declined but persisted long after rejection resolution.

HvG-reactive clones take up long-term residency after rejection resolution

The expression of CD69 and CD103 by CD28+ NKG2D^{Hi} T cells isolated from late rejection biopsies along with the persistence of HvG-reactive clones after resolution of rejection suggested that HvG-reactive clones took up long-term residency within the graft. Remarkably, HvG-reactive clones seeded the entire intestinal tract, including the native colon, with roughly the same frequency of HvG-reactive clones in the transplanted and non-transplanted colon segments (Fig. S8A)(*18*). This observation, combined with the high level of overlap of HvG clones from ileal biopsies taken from different locations at different times, suggests that HvG-reactive clones replenished the total gut-resident T_{RM} compartment, possibly after activation in lymphoid tissues. Apparently this seeding was independent of the local presence of alloantigens(*18, 19*). Nevertheless, it seemed possible that repetitive allogeneic stimulation in the graft would make the same HvG-reactive clones more likely to persist over time and across different graft sites compared to non-HvG clones. We thus compared the clonal overlap between HvG and non-HvG clones identified from two late biopsies taken concurrently from the native and transplanted colon with T cell clones detected in the graft at the time of rejection. HvG clones isolated from the transplanted, in contrast to the native, colon segment displayed a greater overlap with those in ileum and grafted colon at an earlier time point compared to non-HvG-reactive clones (Fig. S8B). These data suggest that continual donor antigenic stimulation in both lymphoid tissues and

the graft may account for a greater expansion, recruitment and persistence of HvG-reactive than non-HvG-reactive recipient clones in the graft.

Intra-graft expansion of GvH clones associated with low donor cell replacement in the graft

Passenger lymphocytes from intestinal transplants can cause GVHD(*3*). However, the origin within the graft and site of activation of these GvH-reactive T cells is unknown. GvH clones were identified as described(*17*) and tracked in post-transplant biopsies (Fig. 5A-B, Table S4). In all early biopsies in 6 of 6 patients (POD9 to POD27), GvH-reactive clones were markedly enriched, compared to pre-transplant donor spleen, among the clones identifiable as donor-derived (Fig. 5B). The greatest GvH clonal enrichment in CD4+ cells was found in the three patients (7, 13 and 15) in whom the replacement rate of graft donor T cells by recipient cells was the slowest (Fig. 1F, 5B and S3). The decline in HvG clones after rejection resolution in Patients 7 and 13 (Fig. 4A) was associated with a reversal of the HvG to GvH clonal ratio (Fig. 5C and 5D). In contrast, the progressive disappearance of donor cells in the other patients (Pt 9,10,14) was associated with increased HvG to GvH clonal ratios (Fig. 5C).

In patients 7, 13 and 15, in whom donor cells long persisted in the graft, GvH-reactive clones mapped in the first biopsy were more likely to persist over time than non-GvH donor-mappable clones (Fig. 5E and S9A). Additionally, the median frequency of individual GvH clones was significantly greater than that of non-GvH clones in early biopsies (Fig. 5F and S9B), in contrast to pre-transplant donor spleens. These results suggest that GvH clones accumulated in the graft in an alloantigen-driven manner.

Graft-resident GvH-reactive clones expand from pre-existing T_{RM}

T_{RM} clones pre-existing in the graft might be expected to have a circulating memory counterpart in draining and remote lymphoid tissues(*18*). In contrast, GvH clones derived from naïve T cells that are primed in the graft following transplant would pre-exist only in gut-associated lymphoid tissues such as mesenteric lymph nodes(*18*). We therefore identified and compared clones present both in donor MLN and spleen with those detected in the MLN or spleen alone in the two donors (Patients 13 and 10) from whom both tissues were available (Fig. 6 and S10). A far greater proportion of clones originally detected in both donor spleen and MLN than of clones detected in only one of these tissues pre-transplant were detectable in post-transplant biopsy specimens (Fig. 6B and S10B). The clonality was low and comparable for CD4 and CD8 TCRs detected in the MLN alone, as is characteristic of naïve cells, whereas the clonality of CD8 cells was higher than that of CD4 cells for clones detected in both spleen and MLN (Fig. 6C and S10C), as is typical for memory cells. Although clones also detected in the spleen accounted for a minority of the MLN clones, they made up roughly 40 to 80% of the CD8+ donor clones detected in the biopsies (Fig. 6D and S10D) and were thus likely tissue-resident memory clones with a recirculating counterpart at the time of transplantation.

Rapid graft infiltration by recipient-derived CD14+ myeloid cells

The expansion of GvH-reactive T cell clones in the graft raised the question of the source of recipient antigen in the donor allograft. Whenever sufficient cell yields were obtained, we analyzed the origin of lamina propria APC populations, the majority of which were CD14+ CD11c+ myeloid cells that also expressed CD33, CD11b and HLA-DR (Fig. 7A). Remarkably, these were very rapidly replaced by recipient-derived cells, which accounted for up to 75% of this subset as early as 10 days post-transplant (Fig. 7B-D). This early replacement of myeloid APCs is quite uniform between patients, regardless of the rate of recipient T cell replacement. Indeed, paired comparison of recipient chimerism between T-cell and CD14+ myeloid-cell populations showed significantly greater recipient chimerism in myeloid cells (Fig. 7C), demonstrating rapid turnover of CD14+ myeloid populations within the graft.

Discussion

The small bowel mucosa of a healthy human adult is estimated to contain more than 30 billion memory T cells(*20*). Rodent experiments have shown that intestinal IELs do not equilibrate with circulating T cells and have low turnover rates(*9*), but turnover studies of mucosal lymphocytes in allogeneic settings are largely lacking in humans. Our study examines the dynamics of this turnover in detail and provides evidence that two-way alloreactivity has a dramatic impact on the rate of recipient T cell replacement in the graft mucosa following intestinal transplantation in humans. TCR tracking data demonstrate remarkable stability of the ileal αβ T cell repertoire over time and space as long as gut-resident CD69+ T cells remain of the same origin (donor or recipient). Notably, mixed rejection, which includes an antibody-mediated component, was associated with accelerated replacement of donor αβ TCR+ T cells in the graft. These data show that vigorous antibody- and cell-mediated HvG responses lead to the clearance and early replacement of the donor lymphocytes in the graft. While human skin T_{RM} are spared from circulating cytotoxic antibodies because of the lack of cellular mediators of antibody-dependent cellular cytotoxicity (ADCC)(*21*), human gut contains CD16-expressing NK cells, which may be cytotoxic under inflammatory conditions(*22*). Thus, the accelerated clearance of donor graft-resident T cells through ADCC mechanisms might take place in the graft itself. Alternatively, but not exclusively, donor cells bound by DSA might be eliminated from the MLN, where the priming of the HvG T-cell response takes place(*10*).

So far, studies of graft-infiltrating T cells have been limited by the lack of reliable tools to distinguish donor-specific T cells from those recruited in a bystander inflammatory response. Studies in a rodent sponge allograft model have led to the suggestion that donor-specific T cells in fact represent only a small proportion of graft-infiltrating cells(*13*). In contrast, our study, which specifically tracks the presence of pre-identified donor-reactive TCR, shows that donor-specific clones account for up to 80% of the T cells identifiable as recipient-derived in rejecting intestinal allografts, overturning long-standing dogma that most graft-infiltrating lymphocytes are “bystanders”. At the times of rejection, we detected a large population of CD28+ NKG2D^{hi} CD8+ cells among recipient-, but not donor-derived IELs, associated with increased expression by epithelial cells of the well-characterized NKG2D ligand MICA, which senses cellular stress. Besides celiac disease, in which the

NKG2D/MICA axis has emerged as a major pathogenic pathway(*15, 16*), NKG2D has been implicated in alloimmune-driven intestinal epithelium damage in rodent models(*23*). Our data now implicate it in human allograft rejection.

Recipient T cells in the graft ultimately acquired CD69 expression and displayed a stable repertoire over time, two hallmarks of T_{RM}(*6, 14*). Notably, a significant proportion of recipient-derived T_{RM} repopulating the graft had HvG-reactive TCR. The limited number of cells available from small forceps biopsies did not allow us to assess the graft-resident lymphocytes in functional assays. It is thus possible that immunosuppression or a "physiological" increase in TCR activation threshold(*24*) prevented graft-residing HvG-reactive T cell activation at steady state. Consistent with this hypothesis, long-term graft-resident recipient CD8 cells down-regulated CD28 and NKG2D, and this downregulation may contribute to the increased activation threshold observed for IEL. However, establishment of a local HvG-reactive T cell repertoire poses a constant threat to the allograft that could reactivate in the context of inflammatory triggers. Following the loss of CD28 and NKG2D and acquisition of CD103 and CD69 by recipient CD8 T cells that adopted the tissue-resident phenotype, the observed reacquisition of CD28 and high levels of NKG2D with retention of CD69 and CD103 by recipient CD8+ IELs during late rejections suggests that tissue-resident CD8 cells can dynamically upregulate CD28 and NKG2D during rejection.

Colonization of the native colon by HvG-reactive clones is consistent with the concept from rodent studies that, following activation in mesenteric lymph nodes and spleen, a subset of memory T cells expresses gut-homing molecules and seeds the entire intestinal tract, independent of cognate antigen(*19*). Broad tissue localization by resident memory T cells was also recently demonstrated in mouse and human skin(*18*). In addition to recruiting new memory cells from the circulation(*25*), there is also some evidence that T_{RM} can expand locally through proliferation in response to cognate antigen stimulation(*26*). However, the extent of this proliferation remains unclear(*27*). In three patients with long-persisting donor T cells in the graft, GvH clones, which were significantly enriched compared to pretransplant lymphoid tissues, were far more likely to overlap than non-GvH clones across two graft samples. This observation suggests that intra-graft stimulation led to intra-graft expansion of GvH clones, accounting for their greater persistence across time points and graft biopsy sites.

Studies in mice have shown early emigration and recipient replacement of graft dendritic cells(*28, 29*). Consistent with a similar mechanism, donor-derived CD14+ myeloid cells were rapidly replaced by their recipient counterparts in intestinal transplant recipients, to a much greater extent than lymphoid populations at the same early time points. The early entrance of recipient-derived APCs seems to induce local activation and expansion of donor GvH-reactive clones. As we did not systematically include HLA-DR in the myeloid panel, we cannot exclude that some of the CD14+ myeloid cells were HLA-DR^{low}, a hallmark of human Myeloid Derived Suppressor Cells (MDSC) that could restrain the two-way immune response. MDSCs have indeed emerged as an important immunoregulatory population, including in inflammatory bowel disease(*30*). Long-term persistence of donor cells in the

graft was associated with decreased HvG to GvH clone ratios, raising the possibility that GvH-reactive clones may selectively attack recipient T cells, restraining the HvG response.

We took advantage of the availability of spleen and MLN in two donors to investigate the origin of donor-mappable clones found in post-transplant biopsies. Donor clones identified in both spleen and MLN were more likely to be found in post-transplant biopsies than those found in spleen or MLN alone. The lower clonality of CD4 vs CD8 T cell populations, which has been shown to be characteristic of memory but not naive human T cells(*31*), suggested that the former were enriched for memory cells, whereas the latter may be enriched for naïve T cells. T_{RM} clones have been shown to have circulating counterparts (T_{CM}) in draining and remote lymphoid tissues in mice(*18*). Similarly, our study showed that a large proportion of donor-derived intestinal clones shared the same TCR as recirculating memory clones detected in both donor spleen and MLN. Thus, we conclude that many graft-resident GvH-reactive clones preexisted as circulating memory clones before transplantation. Moreover, GvH-reactive clones were very stable over time, another characteristic of T_{RM}.

Our study was limited by the relatively low number of patients, an issue inherent to intestinal transplantation. This caveat precluded assessment of the utility of HvG-reactive clone tracking as a biomarker or predictor of rejection. In addition, our method did not permit assessment of the role of HvG-reactive clones generated *de novo* after transplantation in graft infiltration. Thus, our strategy may underestimate the post-transplant HvG response, especially in children with high thymic output.

In conclusion, our study provides insights into the role of two-way alloreactivity in driving human intestinal allograft repopulation by recipient cells. We demonstrated that HvG-reactive clones accumulated in intestinal allografts at the time of rejection, but also persisted long after resolution, despite clonal contraction. These HvG-reactive T_{RM} may be reactivated later to cause rejection. In the absence of overwhelming cellular and antibody-mediated HvG reactivity, preexisting donor T_{RM} with GvH reactivity may expand in the graft and prevent the replacement of donor cells by recipient T cells. Our study suggests that resident memory T cells can mount an immune response that counteracts rejection. Therapeutic approaches to prevent the entry of HvG-reactive T cells and hence their establishment as T_{RM} could potentially have a major impact on outcomes of transplants with large mucosal T_{RM} compartments, such as lungs and intestines.

Materials and Methods

Study Design

Twelve consecutive small intestinal transplant (either isolated or as part of a multivisceral allograft) recipients, engrafted between November 2011 and November 2015 at our institution, were prospectively enrolled into a non-interventional cohort study. The study primarily aimed at correlating intra-graft recipient chimerism and local alloreactive immune responses with clinical outcomes. Nine of them (Pts 4, 5, 6, 7, 9, 10, 13, 14, 15) were enrolled at the time of the transplantation and were monitored until last-follow-up (data cut-off in May 2016). Three additional patients (Pts 8, 11 and 12), who had received a transplant

in other centers, were included late after the transplantation. Pt12 was excluded from the study because of the lack of suitable anti-HLA allele mAb to distinguish recipient from donor cells.

Approval was obtained from the Columbia University Institutional Review Board (IRB# AAAJ5056 and IRB#AAAF2395). All subjects or legal guardians provided their written, informed consent. When intestinal transplant recipients underwent protocol or "for cause" biopsies, excess fresh biopsy specimens were either immediately processed (into single cell suspension) or frozen and stored.

HLA-specific staining and cellular staining

Monoclonal HLA-specific antibodies that readily distinguished donor from the pre-transplant recipient peripheral blood or spleen mononuclear cells were included in lineage-specific panels of antibodies (Table S1, Figure S11), as previously reported(*4*). More information about the multicolor T-cell panel and flow data analysis is provided in the Supplementary Materials.

CFSE-Mixed lymphocyte reactions (MLRs) and cell sorting

These were performed as described(*17*). More details are provided in the Supplementary Materials. DNA was frozen down at −20°C and shipped on dry ice to Adaptive Biotechnologies (Seattle, WA) for high-throughput TCR sequencing. The TCR sequencing data were retrieved from Adaptive's Immunoseq software.

Identification and tracking of HvG and GvH-reactive clones

The initial steps of the analysis are described in the Supplementary Materials. Alloreactive clones were defined by five-fold or greater expansion in stimulated compared to un-stimulated pre-transplant cells, and by minimum frequency of 0.001% in $CFSE^{lo}$, which serves to ensure 85% repeatability, as determined by power analysis (*17*). This ensures that a clone appearing only in $CFSE^{lo}$ without a match in unstimulated sample, considered infinitely expanded by the five-fold expansion criterion, and therefore alloreactive, is sufficiently high-frequency to be re-captured in a repeated MLR. We experimentally observe stabilization of captured alloreactive clone counts and cumulative frequency at this frequency threshold, especially for $CFSE^{lo}$ clones that are relatively low-frequency but still have a nonzero match in unstimulated sample from which they are five-fold expanded, many of which are discounted by a more stringent minimum frequency.

Diversity measures are calculated for total clones and alloreactive clones in all samples, including entropy (H ≡ Σpi log2(pi)), where pi is the frequency of clone i, the related clonality (S ≡ 1 −Hobs/Hmax), and Simpson's index (D ≡ Σpi^2) which is more sensitive to changes in frequency of dominant clones. Clonality, which ranges from 0 to 1, is primarily used, such that higher clonality indicates less diversity, and a less polyclonal distribution. Pair-wise Jensen-Shannon Divergence is calculated as

$$JSD = entropy\left(\frac{p + q}{2}\right) - \frac{entropy(p) + entropy(q)}{2}$$ to indicate overlap

between biopsies for all patients, where JSD of 0 indicates complete overlap, and JSD of 1 complete divergence(*32*).

Contingency tables of clone counts are created to compare biopsies to pre-transplant and to each other, with the total clone count N mappable to pre-transplant MLR in un-stimulated sample, stimulated sample, or both, and subset A of N clones that are alloreactive. These are used in Fisher's Exact Tests of (N1-A1,A1 : N2-A2,A2), and odds ratios with 95% confidence interval are calculated for alloreactive clone fraction between the two samples being compared, along with p-value for the comparison. Cumulative frequencies f(N) and f(A) are also reported for these clonal populations, without associated p-values, as these cannot be straightforwardly derived without repeated MLR.

Supplementary Material

Refer to Web version on PubMed Central for supplementary material.

Acknowledgements

We thank Ms. Jennifer Colozzi for assistance with the submission. We are in debt to Pr. Nadine Cerf Bensussan for helpful review of the manuscript. The authors are also grateful to Ms. Monica Velasco and Dr. Tamas Gonda for their care of intestinal/multivisceral transplant recipients.

Funding: JZ was supported by Fulbright, Monahan foundation, Société Francophone de Transplantation and Schaefer research scholarships. JT was supported by NIH F31AG047003. SDW was supported by a Kidney Research Student Scholar Grant from the American Society of Nephrology. The study was funded by the Schaefer research scholar program and NIAID grant P01 AI106697. The LSRII FACS analyzer used in this study was purchased with NIH award 1S10RR027050-01A1. This work was made possible in part by samples made available through the generous support of Vivienne and Steven Segal for the CCTI Biobank.

References

1. Abu-Elmagd KM, Wu G, Costa G, Lunz J, Martin L, Koritsky DA, Murase N, Irish W, Zeevi A. Preformed and de novo donor specific antibodies in visceral transplantation: long-term outcome with special reference to the liver. American journal of transplantation : official journal of the American Society of Transplantation and the American Society of Transplant Surgeons. 2012; 12:3047–3060.
2. Berger M, Zeevi A, Farmer DG, Abu-Elmagd KM. Immunologic challenges in small bowel transplantation. American journal of transplantation : official journal of the American Society of Transplantation and the American Society of Transplant Surgeons. 2012; 12(Suppl 4):S2–8.
3. Mazariegos GV, Abu-Elmagd K, Jaffe R, Bond G, Sindhi R, Martin L, Macedo C, Peters J, Girnita A, Reyes J. Graft versus host disease in intestinal transplantation. American journal of transplantation : official journal of the American Society of Transplantation and the American Society of Transplant Surgeons. 2004; 4:1459–1465.
4. Zuber J, Rosen S, Shonts B, Sprangers B, Savage TM, Richman S, Yang S, Lau SP, DeWolf S, Farber D, Vlad G, Zorn E, Wong W, Emond J, Levin B, Martinez M, Kato T, Sykes M. Macrochimerism in Intestinal Transplantation: Association With Lower Rejection Rates and Multivisceral Transplants, Without GVHD. American journal of transplantation : official journal of the American Society of Transplantation and the American Society of Transplant Surgeons. 2015
5. Park CO, Kupper TS. The emerging role of resident memory T cells in protective immunity and inflammatory disease. Nature medicine. 2015; 21:688–697.
6. Thome JJ, Yudanin N, Ohmura Y, Kubota M, Grinshpun B, Sathaliyawala T, Kato T, Lerner H, Shen Y, Farber DL. Spatial map of human T cell compartmentalization and maintenance over decades of life. Cell. 2014; 159:814–828. [PubMed: 25417158]

7. Zhu J, Peng T, Johnston C, Phasouk K, Kask AS, Klock A, Jin L, Diem K, Koelle DM, Wald A, Robins H, Corey L. Immune surveillance by CD8alphaalpha+ skin-resident T cells in human herpes virus infection. Nature. 2013; 497:494–497. [PubMed: 23657257]
8. Holtmeier W, Chowers Y, Lumeng A, Morzycka-Wroblewska E, Kagnoff MF. The delta T cell receptor repertoire in human colon and peripheral blood is oligoclonal irrespective of V region usage. The Journal of clinical investigation. 1995; 96:1108–1117. [PubMed: 7635946]
9. Suzuki S, Sugahara S, Shimizu T, Tada T, Minagawa M, Maruyama S, Watanabe H, Saito H, Ishikawa H, Hatakeyama K, Abo T. Low level of mixing of partner cells seen in extrathymic T cells in the liver and intestine of parabiotic mice: its biological implication. European journal of immunology. 1998; 28:3719–3729. [PubMed: 9842914]
10. Wang J, Dong Y, Sun JZ, Taylor RT, Guo C, Alegre ML, Williams IR, Newell KA. Donor lymphoid organs are a major site of alloreactive T-cell priming following intestinal transplantation. Am J Transplant. 2006; 6:2563–2571. [PubMed: 16952298]
11. Meier D, Docena GH, Ramisch D, Toscanini U, Berardi G, Gondolesi GE, Rumbo M. Immunological status of isolated lymphoid follicles after intestinal transplantation. American journal of transplantation : official journal of the American Society of Transplantation and the American Society of Transplant Surgeons. 2014; 14:2148–2158.
12. Iwaki Y, Starzl TE, Yagihashi A, Taniwaki S, Abu-Elmagd K, Tzakis A, Fung J, Todo S. Replacement of donor lymphoid tissue in small-bowel transplants. Lancet. 1991; 337:818–819. [PubMed: 1707470]
13. Halloran PF. T cell-mediated rejection of kidney transplants: a personal viewpoint. American journal of transplantation : official journal of the American Society of Transplantation and the American Society of Transplant Surgeons. 2010; 10:1126–1134.
14. Sathaliyawala T, Kubota M, Yudanin N, Turner D, Camp P, Thome JJ, Bickham KL, Lerner H, Goldstein M, Sykes M, Kato T, Farber DL. Distribution and compartmentalization of human circulating and tissue-resident memory T cell subsets. Immunity. 2013; 38:187–197. [PubMed: 23260195]
15. Hue S, Mention JJ, Monteiro RC, Zhang S, Cellier C, Schmitz J, Verkarre V, Fodil N, Bahram S, Cerf-Bensussan N, Caillat-Zucman S. A direct role for NKG2D/MICA interaction in villous atrophy during celiac disease. Immunity. 2004; 21:367–377. [PubMed: 15357948]
16. Meresse B, Chen Z, Ciszewski C, Tretiakova M, Bhagat G, Krausz TN, Raulet DH, Lanier LL, Groh V, Spies T, Ebert EC, Green PH, Jabri B. Coordinated induction by IL15 of a TCR-independent NKG2D signaling pathway converts CTL into lymphokine-activated killer cells in celiac disease. Immunity. 2004; 21:357–366. [PubMed: 15357947]
17. Morris H, DeWolf S, Robins H, Sprangers B, LoCascio SA, Shonts BA, Kawai T, Wong W, Yang S, Zuber J, Shen Y, Sykes M. Tracking donor-reactive T cells: Evidence for clonal deletion in tolerant kidney transplant patients. Science translational medicine. 2015; 7:272ra210.
18. Gaide O, Emerson RO, Jiang X, Gulati N, Nizza S, Desmarais C, Robins H, Krueger JG, Clark RA, Kupper TS. Common clonal origin of central and resident memory T cells following skin immunization. Nature medicine. 2015; 21:647–653.
19. Masopust D, Choo D, Vezys V, Wherry EJ, Duraiswamy J, Akondy R, Wang J, Casey KA, Barber DL, Kawamura KS, Fraser KA, Webby RJ, Brinkmann V, Butcher EC, Newell KA, Ahmed R. Dynamic T cell migration program provides resident memory within intestinal epithelium. The Journal of experimental medicine. 2010; 207:553–564. [PubMed: 20156972]
20. Ganusov VV, De Boer RJ. Do most lymphocytes in humans really reside in the gut? Trends in immunology. 2007; 28:514–518. [PubMed: 17964854]
21. Watanabe R, Gehad A, Yang C, Scott LL, Teague JE, Schlapbach C, Elco CP, Huang V, Matos TR, Kupper TS, Clark RA. Human skin is protected by four functionally and phenotypically discrete populations of resident and recirculating memory T cells. Science translational medicine. 2015; 7:279ra239.
22. Leon F, Roldan E, Sanchez L, Camarero C, Bootello A, Roy G. Human small-intestinal epithelium contains functional natural killer lymphocytes. Gastroenterology. 2003; 125:345–356. [PubMed: 12891535]

23. Karimi MA, Bryson JL, Richman LP, Fesnak AD, Leichner TM, Satake A, Vonderheide RH, Raulet DH, Reshef R, Kambayashi T. NKG2D expression by CD8+ T cells contributes to GVHD and GVT effects in a murine model of allogeneic HSCT. Blood. 2015; 125:3655–3663. [PubMed: 25788701]
24. Cheroutre H, Lambolez F, Mucida D. The light and dark sides of intestinal intraepithelial lymphocytes. Nature reviews. Immunology. 2011; 11:445–456.
25. Schenkel JM, Fraser KA, Vezys V, Masopust D. Sensing and alarm function of resident memory CD8(+) T cells. Nat Immunol. 2013; 14:509–513. [PubMed: 23542740]
26. Cuburu N, Graham BS, Buck CB, Kines RC, Pang YY, Day PM, Lowy DR, Schiller JT. Intravaginal immunization with HPV vectors induces tissue-resident CD8+ T cell responses. J Clin Invest. 2012; 122:4606–4620. [PubMed: 23143305]
27. Schenkel JM, Masopust D. Tissue-resident memory T cells. Immunity. 2014; 41:886–897. [PubMed: 25526304]
28. Celli S, Albert ML, Bousso P. Visualizing the innate and adaptive immune responses underlying allograft rejection by two-photon microscopy. Nature medicine. 2011; 17:744–749.
29. Larsen CP, Morris PJ, Austyn JM. Migration of dendritic leukocytes from cardiac allografts into host spleens. A novel pathway for initiation of rejection. The Journal of experimental medicine. 1990; 171:307–314. [PubMed: 2404081]
30. Haile LA, von Wasielewski R, Gamrekelashvili J, Kruger C, Bachmann O, Westendorf AM, Buer J, Liblau R, Manns MP, Korangy F, Greten TF. Myeloid-derived suppressor cells in inflammatory bowel disease: a new immunoregulatory pathway. Gastroenterology. 2008; 135:871–881. 881 e871-875. [PubMed: 18674538]
31. Qi Q, Liu Y, Cheng Y, Glanville J, Zhang D, Lee JY, Olshen RA, Weyand CM, Boyd SD, Goronzy JJ. Diversity and clonal selection in the human T-cell repertoire. Proc Natl Acad Sci U S A. 2014; 111:13139–13144. [PubMed: 25157137]
32. Putintseva EV, Britanova OV, Staroverov DB, Merzlyak EM, Turchaninova MA, Shugay M, Bolotin DA, Pogorelyy MV, Mamedov IZ, Bobrynina V, Maschan M, Lebedev YB, Chudakov DM. Mother and child T cell receptor repertoires: deep profiling study. Front Immunol. 2013; 4:463. [PubMed: 24400004]

One Sentence Summary

Graft-versus-Host and Host-versus-Graft memory T cells can take up long-term residency in human intestinal allograft mucosa and the dynamics of the two-way alloimmune response correlate with graft outcomes.

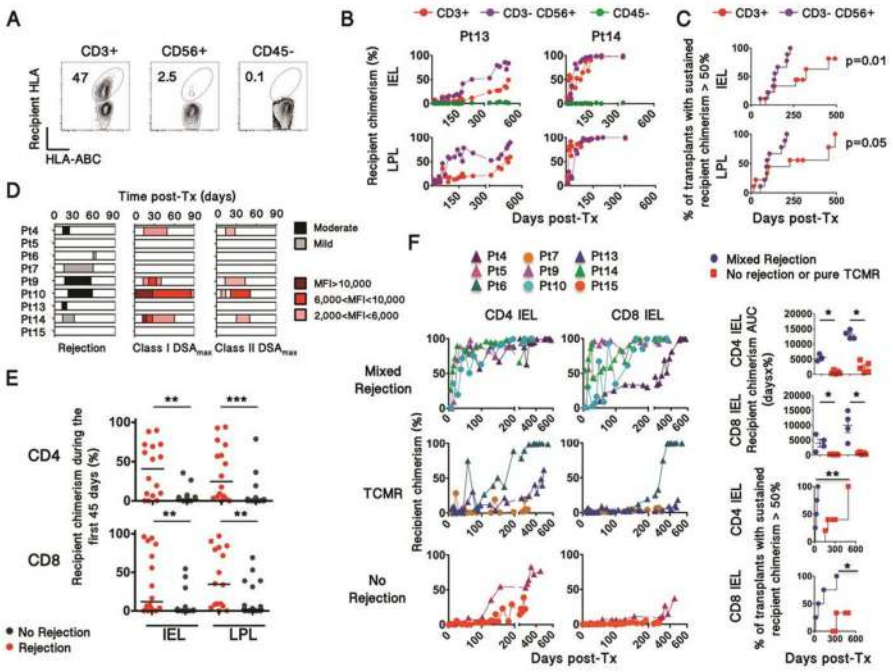

Figure 1. Relationship between rejection and recipient chimerism in intestinal allografts

(**A**) Representative plots (from Patient 14) depicting recipient chimerism in cell subsets isolated from graft biopsies (n=183). Chimerism was detected using recipient HLA allele-specific and pan-HLA class I antibodies. (**B**) Replacement rate of donor CD3+, CD3− CD56+ and CD45− cells by recipient cells (recipient chimerism) over time in IELs and LPLs, isolated from serial protocol biopsies. The 2 selected patients depict different T-cell turnover kinetics. Panels **C, D, E** depict 170 biopsies obtained from 9 patients with a longitudinal follow-up from POD0 to up to POD600. (**C**) Kaplan Meier curves plot the proportion of transplants for which recipient cells permanently exceeds 50% in the indicated cell populations over time. Survival curves were compared using Log-rank (Mantel-Cox) Test. (**D**) Graphic representation showing the severity/intensity and period of rejection episodes (left) and donor-specific antibodies (right) during the first three months post-transplant. MFI, mean fluorescence intensity. DSA, Donor-Specific Antibody. (**E**) Recipient chimerism in CD4 and CD8 IEL and LPL within the first 45 days (Mann-Whitney U test; ** $p<0.01$, *** $p<0.001$). (**F**) Recipient chimerism over time in CD4+ and CD8+ αβTCR+ IELs isolated from serial biopsies, according to the occurrence of mixed rejection, TCMR or no rejection. Dots and triangles represent multivisceral transplant and isolated intestinal transplant recipients, respectively. AUC, Area Under the Curve; Pt, Patient; TCMR, T-cell-mediated rejection. Turnover kinetics were assessed by the integration of recipient chimerism over time (AUC) and by the 50% turnover rate (right panels), plotting the proportion of transplants for which recipient cells permanently exceeds 50% in the indicated cell population over time. Survival curves and AUC were compared using Log-rank (Mantel-Cox) and Mann-Whitney test, respectively (* $p<0.05$, ** $p<0.01$).

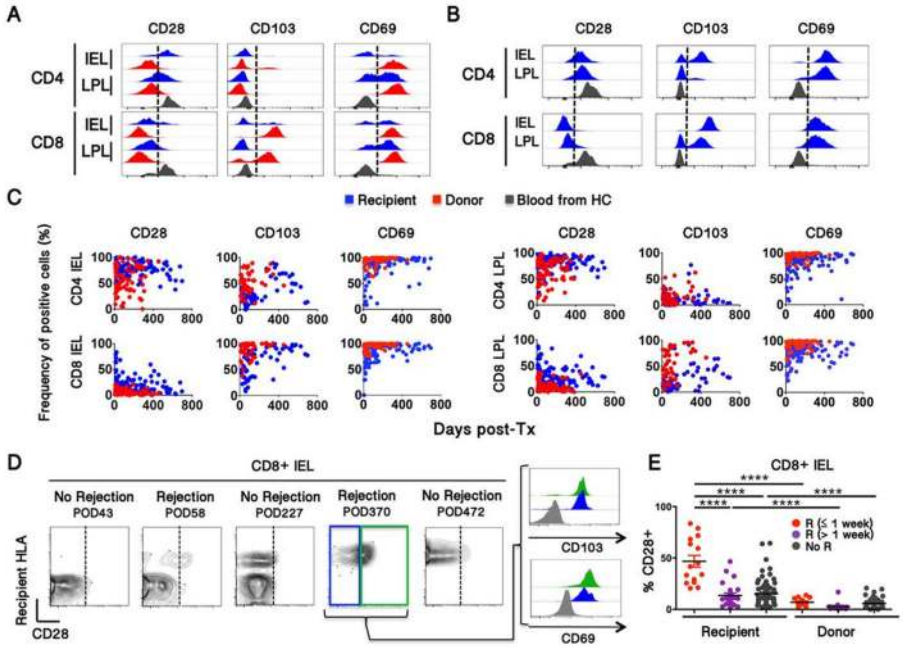

Figure 2. Relationship between recipient intestinal T cell phenotype and rejection

(A, B) Comparison of recipient and donor IEL and LPL T cell subset phenotypes with that of blood T cells. Representative IEL and LPL at early (a) and late (b) time points are shown. **(C)** Evolution of recipient and donor T cell phenotype in IEL (left) and LPL (right) over time. CD28, CD103 and CD69 phenotypic information was available for 127, 83 and 120 biopsies, respectively (**D**) Representative contour plots (from Patient 6) showing CD28 upregulation on recipient but not donor CD8+ IELs during rejection. (**E**) Summary of CD28 expression by recipient CD8 IEL T cells in relationship to rejection episodes. Frequencies of CD28+ cells were compared using Mann-Whitney test (**** $p<0.0001$).

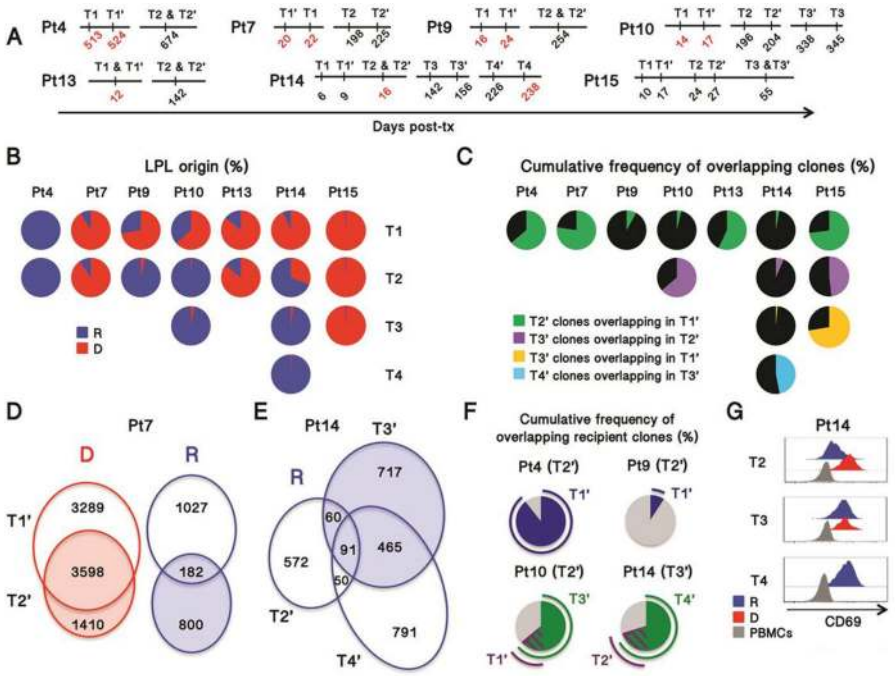

Figure 3. Clonal analysis of recipient T cells in intestinal allografts

(**A**): Timeline for biopsies showing rejection (red) or non-rejection (black) analyzed by multicolor FCM (T1-4) or repertoire analysis (T1'-4') in 7 patients (Pt). (**B**): Frequency of recipient and donor cells in isolated LPL for 7 patients. IEL cell origin, which was almost superimposable with LPL, is shown in Fig. S7. (**C**) Cumulative frequency of T cell clones (defined by TCRβ CDR3 sequences) overlapping in sequential biopsies. (**D**) Venn diagram representing two biopsies (T1' and T2') from Patient 7 showing the number of clones detected in each biopsy alone or in both, according to their donor (D) or recipient (R) origin. (**E**) Venn diagram representing the number of recipient (R) clones overlapping across three biopsies taken from Patient 14 at POD16 (T2'), POD156 (T3') and POD238 (T4'). (**F**) Cumulative frequency of the clones identified in a given biopsy (indicated within the brackets) overlapping in other biopsies taken earlier (blue) (Pt4 and Pt9) or both earlier (purple) and later (green)(Pt10 and Pt14). (**G**) Histograms representing three biopsies taken from Patient 14. R, recipient; D, donor.

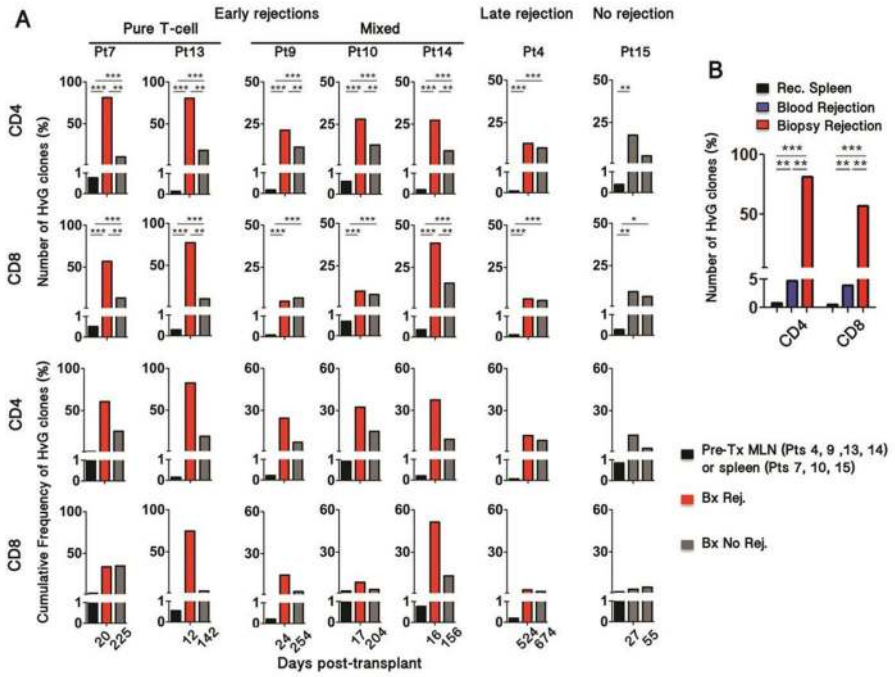

Figure 4. Evolution of host-vs-graft-reactive recipient T cell clones in intestinal allografts

(**A**) Frequency of HvG clones in rejecting biopsies (red) compared to pre-transplant lymph node (Pts 4, 9, 13 and 14) or spleen (Pts 7, 10, 15) samples (black) and non-rejecting biopsies (gray). The denominator includes all the clones that were identified in pre-transplant recipient samples (HvG plus all other clones). HvG clone frequencies were compared using Fischer exact test; *** $p < 10^{-25}$; ** $p < 10^{-10}$; * $p < 10^{-3}$. (**B**) Frequency of HvG clones in the blood (blue) and in the graft (red) at the time of rejection (POD20) compared to pre-transplant spleen sample in Patient 7 (Fischer exact test; *** $p < 10^{-25}$; ** $p < 10^{-10}$). (**C, D**) Subsequent analyses were performed in Patient 4, in whom serial biopsies were performed in ileum and colon.

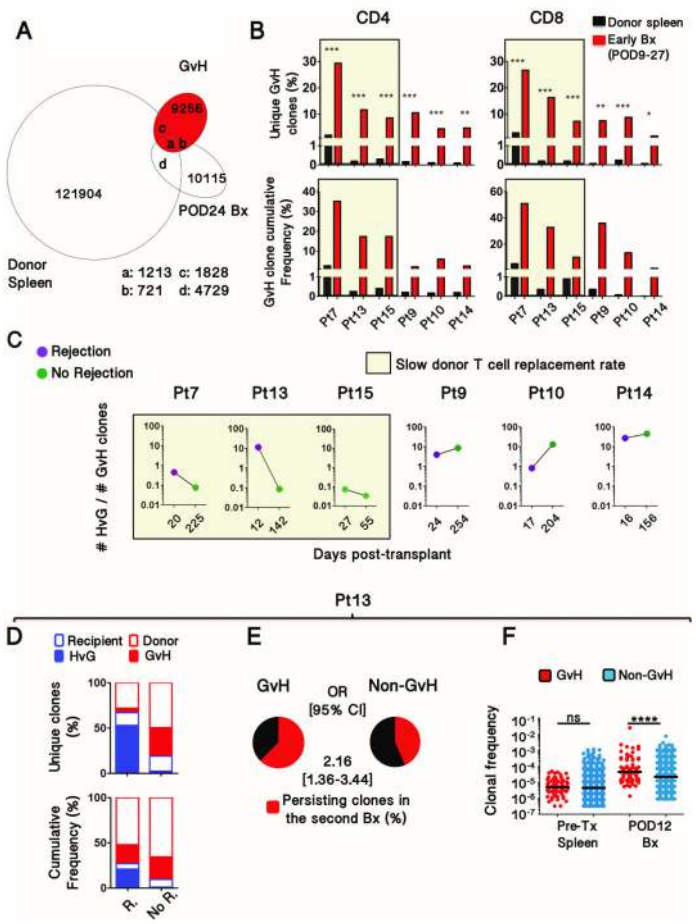

Figure 5. Expansion of GvH clones that may counteract the replacement of donor cells by recipient cells

(**A**) Venn diagram depicting the number of T cell clones overlapping between donor spleen total clones, GvH-reactive clones and clones identified as donor-derived in the POD24 biopsy from Patient 7. (**B**) Frequency of GvH clones in early biopsies (red) compared to pre-transplant donor spleen samples (black). The denominator includes all clones that could be identified in pre-transplant donor samples (Fischer exact test; *** $p < 10^{-25}$; ** $p < 10^{-10}$; * $p < 10^{-3}$). (**C**) Evolution of the HvG to GvH clonal ratio after rejection resolution or in the absence of rejection in all patients for whom both HvG and GvH clones were identified in biopsies.. (**D**) Proportion of HvG and GvH-reactive clones in rejecting (R) and non-rejecting (No R.) biopsies, at POD12 and POD142 respectively, using as denominator the clones identified in pre-transplant recipient or donor samples in Patient 13. (**E**) From the same patient (Pt13), exhibiting a slow donor T cell replacement rate, proportion of GvH and non-GvH clones from early biopsies (POD12) that were detected in subsequent biopsies (POD142). OR, Odds Ratio. In order to permit comparison in the analysis in (F), only GvH clones that were also detectable in the unstimulated populations were used for this analysis. However, analysis that included all GvH clones provided similar results ($p<0.05$), yet with a lower OR (~1.5). (**F**) Comparison of individual clonal frequencies of the GvH and non-GvH clones identified in the early biopsy and pre-transplant samples in Patient 13. Pre-transplant

and post-transplant frequencies were compared using Fischer exact test (**** $p < 10^{-4}$). Horizontal bars represent medians.

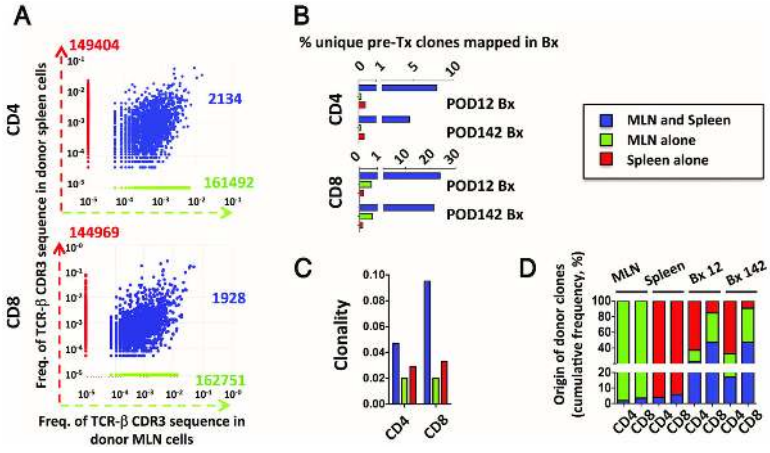

Figure 6. Origin of early detected GvH clones in Patient 13

(**A**) Scatter plots showing donor clones identified in the mesenteric lymph nodes (MLN) alone (green), in the spleen alone (red) and those found in both the mesenteric lymph nodes and spleen (blue) in Patient 13. (**B**) The bar graphs depict the proportion of the three donor-derived cell subsets (green, red and blue) also detected in the post-transplant intestinal biopsies with a sizeable donor population. (**C**) Clonality of CD4 and CD8 clones from the three subsets. (**D**) Proportion of blue, green and red clones among the total donor clones in the MLN, spleen and post-transplant biopsies.

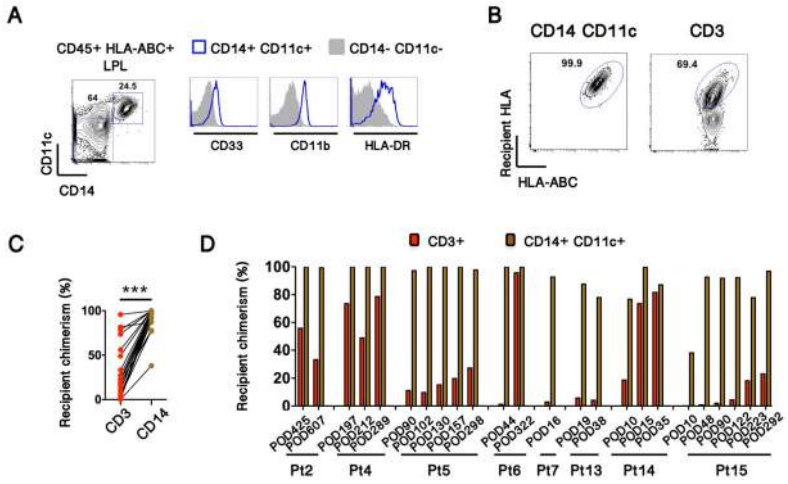

Figure 7. Recipient APCs replace graft APCs early after transplant

(**A**) CD14+ CD11c+ CD45+ lamina propria cells express CD33, CD11b and HLA-DR. (B) Representative contour plots (from Patient 14), showing recipient chimerism in CD14+ CD11c+ myeloid cells and in T cells. (**C**) Comparison of recipient chimerism between myeloid and T cells in individual biopsy specimens (Paired t-test, ***< 0.0001). (**D**) Recipient chimerism over time in CD14+ CD11c+ myeloid cells and CD3+ T cells.